Sustainable Food Technology

ROYAL SOCIETY OF CHEMISTRY

PAPER

View Article Online
View Journal | View Issue

Cite this: *Sustainable Food Technol.*, 2025, 3, 1480

Sustainable oleogel encapsulation of tilapia fish oil using protein-based cryogels: fabrication, characterization, and digestion behavior

Daniel Tua Purba, [a] Jaydeep Dave [b] and Pichayada Somboon *[c]

In this study, a novel cryogel-templated oleogel system was developed by incorporating sustainable tilapia fish oil (STFO-O) into hybrid protein-based cryogels composed of whey protein isolate (WPI), fish gelatin (FG), and tannic acid (TA) as a natural polyphenolic crosslinker. Unlike previous reports on single-phase cryogels or oleogels, this dual-network system synergistically combines the advantages of protein–polyphenol interactions and porous cryogel structures for improved encapsulation, stability, and targeted release of omega-3-rich oils. The tilapia visceral oil extracted using a green deep eutectic solvent–ultrasound-assisted method, exhibited high unsaturated fatty acid content (74.07%), including 31.72% polyunsaturated fatty acids (PUFAs) and 8.47% omega-3 fatty acids, including α-linolenic acid (ALA), EPA, and DHA. The optimized WPI/FG 15 : 5-TA formulation showed excellent oil absorption (42.20 ± 0.20 g g^{-1}) and holding capacity (96.80 ± 0.69%), with a peroxide value of only 2.95 ± 0.14 meq kg^{-1} after 8 days at 30 °C, indicating enhanced oxidative stability. FTIR analysis confirmed hydrogen bonding and successful entrapment of oil within the protein matrix. *In vitro* digestion demonstrated a controlled release profile, with free fatty acid (FFA) release limited to 62.17 ± 2.76% after 120 minutes compared to 83.61 ± 1.42% in the WPI-only control. These results validate the WPI–FG–TA cryogel–oleogel system as a promising and sustainable platform for delivering omega-3-enriched fish oils in functional food and nutraceutical applications.

Received 27th June 2025
Accepted 20th July 2025

DOI: 10.1039/d5fb00322a

rsc.li/susfoodtech

Sustainability spotlight

This study presents a sustainable approach for valorizing tilapia viscera by extracting omega-3-rich oils using green methods and structuring them into oleogels with food-grade cryogels. Utilizing natural proteins (whey protein isolate and fish gelatin) and tannic acid as a bio-based crosslinker, the system offers an edible, biodegradable vehicle for delivering functional lipids. By reducing saturated fats and synthetic additives, this method supports circular bioeconomy goals and aligns with UN SDGs—particularly SDG 12 (Responsible Consumption and Production) and SDG 3 (Good Health and Well-Being).

1 Introduction

The global tilapia industry generates approximately 2.3 million tons of fish annually, with processing waste, including viscera accounting for 30–40% of the total fish weight, representing a substantial yet underutilized resource.[1] Concurrently, omega-3 fatty acid deficiency affects over 2 billion people worldwide, with average dietary intake falling nearly 60% below recommended levels.[2] This dual challenge of aquaculture waste accumulation and micronutrient deficiency highlights the urgent need for sustainable lipid-based delivery systems derived from fish by-products.

Over the past decade, oleogelation has emerged as a promising strategy for structuring liquid oils into semi-solid systems using three-dimensional networks of structuring agents. These oleogels provide not only healthier fat alternatives but reduce saturated and trans fats linked to cardiovascular diseases which also serve as effective carriers for lipophilic bioactives such as omega-3 fatty acids.[3,4] Traditional oleogel systems, often created using direct dispersion of waxes, monoglycerides, or ethyl cellulose at elevated temperatures, pose limitations due to high energy input, synthetic structuring agents, and poor compatibility with heat-sensitive nutrients.[5,6] Recent approaches have sought to overcome these limitations through indirect oleogelation methods such as emulsion-templating, foam-templating, and cryogel-templating, where the oil is introduced into a preformed biopolymer network.[7]

[a]*Program in Food Science and Technology, School of Food Industry, King Mongkut's Institute of Technology Ladkrabang, Bangkok 10520, Thailand*

[b]*Faculty of Medical Technology, Mahidol University, Salaya, Phutthamonthon, Nakhon Pathom 73170, Thailand*

[c]*Program in Fermentation Technology, School of Food Industry, King Mongkut's Institute of Technology Ladkrabang, Bangkok 10520, Thailand. E-mail: pichayada.so@kmitl.ac.th*

Table 1 Comparison of oleogel systems for lipophilic bioactive encapsulation

Oleogel system	Oil absorption ($g\ g^{-1}$)	Oil retention (%)	Oxidative stability	FFA release (%)	Limitations	Reference
Wax-based	15–25	80–85	Moderate	70–80	Synthetic additives and consumer concerns	12
Whey protein isolate (WPI) alone	10–20	75–85	Poor	80–90	Weak structure and poor oil retention	13
Gelatin alone	20–30	85–90	Moderate	75–85	Temperature sensitivity	14
Polysaccharide-based	25–35	80–90	High	60–70	Possible swelling in pH-sensitive environments	15

Despite progress, most reported oleogels rely on single biopolymer systems or synthetic stabilizers. Polysaccharide-based cryogels offer structural advantages but often lack nutritional value, while protein-based oleogels using either whey protein isolate (WPI) or gelatin alone tend to show limited oil entrapment and oxidative stability.[8,9] Moreover, few studies explore the synergistic use of dual-protein matrices in combination with bio-derived polyphenolic crosslinkers such as tannic acid (TA).[10,11] Tannic acid, with its abundant phenolic hydroxyl groups, can form strong hydrogen bonds with proteins, enhancing structural rigidity while contributing antioxidant properties.

This study addresses these gaps by introducing a novel protein–polyphenol cryogel platform based on WPI, fish gelatin (FG), and TA to encapsulate omega-3-rich tilapia visceral oil (TVO). A green extraction approach utilizing natural deep eutectic solvents (DESs) coupled with ultrasonication was employed to obtain high-quality oil containing 31.72% polyunsaturated fatty acids (PUFAs) and 8.47% omega-3 fatty acids. The dual-network cryogels created from WPI/FG crosslinked with TA were used as templates to fabricate oleogels by capillary infusion of oil. Compared to traditional single-network systems, this dual-protein system aims to improve oil loading, oxidative stability, and digestion-triggered release behavior. To position our work in the broader context, Table 1 summarizes representative cryogel- and oleogel-based delivery systems from the literature, highlighting their composition, encapsulation efficiency, and digestion behavior.

Therefore, this study not only explores the structural and functional characteristics of WPI–FG–TA cryogels but also investigates their potential as sustainable matrices for stabilizing and delivering omega-3-rich lipids in functional foods and nutraceutical systems. By addressing the structural limitations of previous systems and leveraging underutilized fish by-products, this work provides a comprehensive solution bridging sustainability, nutrition, and food engineering.

2 Materials and the methodology

2.1 Materials

This study used fresh tilapia viscera sourced from the Huatake Market located in Ladkrabang, Bangkok, Thailand. Fish gelatin (FG) and whey protein isolate (WPI) were used as primary ingredients to develop cryogel particles aimed at stabilizing omega-3 fatty acids. The fish gelatin, supplied by Halamix International (Bangkok, Thailand), had a high gel strength of 275, protein content of 90%, and a particle size of 20 mesh. The whey protein isolate, sourced from Now Foods Thailand (Bangkok, Thailand), contained 94% protein on a dry weight basis, with minimal lactose (0.2%) and ash (2.0%) content. Tannic acid was obtained from Sigma-Aldrich (St. Louis, MO, USA).

Fish oil extraction was successfully performed with sustainable extraction methods using a combination of natural deep eutectic solvent and ultrasonication,[16] producing an oil with a notable total unsaturated fatty acid content of 74.07%. This study will explore how the fabrication of oleogel-structured composites with cryogel particles, enriched with omega-3 fatty acids of 8.47% from tilapia visceral oil impacts stability and bioavailability.

2.2 Methodology

2.2.1 Extraction of oil from tilapia viscera. Natural deep eutectic solvent was prepared by mixing urea and choline chloride (1 : 2 w/w) and heating at 80 °C with stirring until a homogeneous mass formed with slight modification.[17] The DES was then diluted with water (3 : 2 v/v) to get the aqueous solution used for oil extraction. 100 g of minced tilapia viscera was mixed with DES (1 : 0.5 w/w) and subjected to either homogenization (13 000 rpm) or ultrasonication (80% amplitude) for 15 min. The treated mixture was heated at 80 °C for 15 min, filtered, and centrifuged (3000 g, 15 min, 25 °C) to separate the oil phase. The extracted tilapia viscera oil (TVO) was collected for further analysis.

2.2.2 Preparation of hydrogels. Fish gelatin and whey protein hydrogels were prepared using a modified method based on prior studies with modifications.[18] A whey protein isolate (WPI) solution was prepared by dissolving in deionized water with continuous stirring at room temperature for 24 hours, while the FG solution was prepared by stirring at 50 °C to ensure complete dissolution.[19] Tannic acid (TA), a natural polyphenolic as a crosslinker, and fish gelatin (FG), and whey protein isolate (WPI) in different amounts were used to create six hydrogel formulations. To examine the synergistic effects of biopolymer composition on the structural properties of the resulting hydrogel matrices, these formulations were developed. Formulations included (1) hydrogel containing only 20% WPI; (2) hydrogel containing 10% WPI and 10% FG; (3) crosslinked hydrogel consisting of 20% WPI and 1% TA; (4) crosslinked hydrogel consisting of 18% WPI, 2% FG, and 1% TA;

(5) cross-linked hydrogel consisting of 15% WPI, 5% FG, and 1% TA; and (6) cross-linked hydrogel containing 10% WPI, 10% FG, and 1% TA. All percentages were given in (w/v) according to the mass of the total hydrogel and created in triplicate. The pH of the solutions was increased to 6.5 to enhance strong electrostatic interactions, based on the pH ranges of WPI (4.6–5.6) and FG (7–9).[20] Adjustments were made using 1.0 M HCl and 1.0 M NaOH. The cross-linker was added to create crosslinking of protein–polyphenol interactions and stirred at 600 rpm in a 50 °C water bath.[21] About 40 mL of each mix was poured into 50 mL plastic tubes (2.5 cm diameter), heated at 90 °C for 20 minutes to trigger gelation, and then chilled quickly in ice water for 15 minutes. The obtained protein gel was cooled, and then blended with a high-speed mixer running at 13 000 rpm for 3 minutes. This was followed by 1 minute of ultrasonication (Sonics & Material Vibra-Cell model) set at 80% amplitude to tighten the network. They were then chilled at 4 °C overnight to set before being sliced into 2 cm-high and 2.5 cm-diameter cylindrical pieces for further processing.

2.2.3 Preparation of cryogel particles. The hydrogels were poured into aluminum containers, frozen at −40 °C for 45 minutes in a blast chiller (FAB25, Electrolux, Italy), and freeze-dried in a Kinetic LD0.5 freeze dryer (Kinetic Engineering Co., Ltd). The freeze-drying process followed a controlled cycle: 20 minutes at −30 °C, 24 hours at −20 °C, 24 hours at −10 °C, 8 hours at 0 °C, 16 hours at 10 °C, and 8 hours at 20 °C under a vacuum of 0.2 mbar. The particles were stored in a desiccator at room temperature until further use. The freeze-drying cycle was designed to ensure complete ice sublimation while preserving pore structure integrity.[22] The temperature gradually increases from −30 °C to 20 °C to prevent pore collapse that can occur with rapid temperature changes. The extended time at each temperature allows for complete sublimation of ice crystals of various sizes, with smaller crystals subliming at higher temperatures.

2.2.4 Micromorphology analysis. A field emission scanning electron microscope was applied to show the cryogel microstructure. The sample cross-section was coated with gold and imaged by using a 10 kV acceleration voltage microscope using FE-SEM (Apreo S; Thermo Fisher Scientific).[8]

2.2.5 Bulk density and porosity of the cyrogel. The bulk density of the WP cryogel particles was determined by gently filling a graduated cylinder with the particles and weighing them. The bulk density was calculated using the particle mass (m) and the bulk volume of the sample (V_b), as shown in eqn (1).[8]

$$\text{Bulk density} = \frac{m}{V_b} \quad (1)$$

The porosity (%) of the cryogel powder was calculated using the equation.[23]

$$\text{Porosity } (\%) = 1 - \frac{\rho_b}{\rho_t} \times 100 \quad (2)$$

where ρ_b (g cm^{-3}) is the bulk density of the powder. ρ_t (g cm^{-3}) is the true density of the material, with ρ_t considered to be 1.35 g cm^{-3} for WPI, 1.35 g cm^{-3} for fish gelatin, and 2.12 g cm^{-3} for tannic acid.[21]

2.2.6 Preparation of fish oil-loaded cryogel particles. Oil-loaded cryogel composites were prepared by weighing 10 g of cryogel particles composed of whey protein and fish gelatin, based on an adapted method.[20] Tilapia fish oil (TFO) was gradually added dropwise to loading oil contents ranging from 57–77% (w/w). The mixtures were homogenized using an Ultra-Turrax at 10 000 rpm for 2 minutes. The obtained oleogel-structured composites were then evaluated for their physicochemical properties, stability, and *in vitro* digestion behavior.

2.2.7 Firmness and color of oleogels. The firmness of the oleogels was measured by an uniaxial compression test using a texture analyzer (TA.XT Plus, Stable Micro Systems Ltd, Godalming, UK), and for this aim, an accurate volume of oleogel (2 mL) was transferred to a 5 mL glass beaker and compressed for 30 s with a 5 g-cylinder. The oleogel was then analyzed using a 5 mm diameter cylindrical probe mounted at a 25 mm min^{-1} crosshead speed. Force–distance curves were obtained from the compression tests, and firmness was taken as the maximum force (N) required to penetrate the sample by 2 mm.[20]

The color properties were evaluated using a Chroma Meter CR-400 (Konica-Minolta, Osaka, Japan). Prior to taking measurements, the equipment was calibrated with the manufacturer's standard white reference tile. Color values were recorded as L^* (lightness, 0 = black to 100 = white), a^* ($-a$ = green to $+a$ = red), and b^* ($-b$ = blue to $+b$ = yellow). Each sample was placed against a white background with uniform lighting, and six readings were collected from it. The experiment was repeated three times, giving a total of 18 measurements per treatment. The data are presented as the mean ± standard deviation.[24]

2.2.8 Oil absorption capacity (OAC). The initial weight of the cryogel samples was measured using an analytical balance. The samples were then immersed in fish oil for 10 hours to allow oil absorption to reach equilibrium and form oleogels. The 10 hour immersion time was optimized through preliminary studies (data not shown) testing intervals from 1 to 24 hours. Oil absorption reached equilibrium after 8 hours, with no significant increase observed beyond 10 hours, confirming optimal absorption conditions. After the immersion period, the samples were removed from the oil bath and allowed to drain naturally by suspending them for 20 seconds to eliminate excess surface oil. Following this, the samples were reweighed. The oil absorption capacity (OAC) was calculated using the following equation:[21]

$$\text{OAC } (\text{g g}^{-1}) = \frac{M - M_0}{M_0} \times 100 \quad (3)$$

where M_0 is the initial dry weight of the cryogel (g), and M is the weight of the sample after oil absorption and surface draining (g).

2.2.9 Oil holding capacity (OHC). The oil holding capacity (OHC) of the oil/WP cryogel particles was measured by placing about 1 g of the sample in a microcentrifuge tube.[8] The sample was centrifuged at 10 000 rpm for 15 minutes at 20 °C using a Mikro 120 centrifuge (Hettich Zentrifugen, Germany). After

centrifugation, the excess oil was poured off, and the sample was weighed. The OHC was calculated as the percentage of oil retained in the sample after centrifugation.

Oil holding capacity (OHC) was determined based on the method of Li *et al.*[21], and oleogels were placed in 50 mL centrifuge tubes lined with absorbent paper and centrifuged at 16 000 rpm for 20 minutes. OHC was calculated using the following equation:

$$\text{OHC } (\text{g g}^{-1}) = \frac{M_1}{M} \times 100 \quad (4)$$

where M and M_1 represent the amount of fish oil in the oleogel before and after centrifugation, respectively; this analysis indicates the oil retention ability of the oleogels under centrifugal force.

2.2.10 Oxidative stability of oleogels. Oxidative stability of STFO-O was determined through measurement of the peroxide value (PV) at a storage temperature of 30 ± 1 °C. Oleogel samples were stored in tightly closed amber glass bottles and were analyzed at days 0, 2, 4, 6, and 8 to monitor lipid oxidation. The PV was determined according to the method of Takeungwongtrakul *et al.* with slight modifications.[25] The powder (0.2 g) was suspended in 5 mL of distilled water. Then the mixture was stirred for 5 min to allow complete dispersion. To 1 mL of the mixture, 2 mL of chloroform/methanol (2 : 1, v/v) were added and mixed using a vortex mixer for 3 s to separate the sample into two phases. The organic solvent phase (50 mL) was mixed with 2.35 mL of chloroform/methanol (2 : 1, v/v), followed by 50 mL of 30% ammonium thiocyanate (w/v) and 50 mL of 20 mM ferrous chloride solution in 3.5% HCl (w/v). After 20 min, the absorbance of the colored solution was read at 500 nm using a spectrophotometer (Shimadzu, Kyoto, Japan). The blank was prepared in the same manner, except that distilled water was used instead of ferrous chloride. The PV was calculated after blank subtraction and expressed as mg cumene hydroperoxide per g oil. A standard curve was prepared using cumene hydroperoxide with a concentration range of 0.5–2 ppm.

2.2.11 Fourier-transform infrared spectroscopy (FTIR). Fourier-transform infrared spectroscopy (FTIR) was used to identify specific interactions between the crosslinked agent, WPI, FG, and fish oil. The FTIR spectra of the extracted oils were acquired using an ATR-FTIR model Equinox 55 (Bruker, Ettlingen, Germany) within the range of 400–4000 cm^{-1}, employing a resolution rate of 4 cm^{-1}.[4]

2.2.12 *In vitro* simulated digestion. The digestion pattern of the oleogel samples was assessed using a simulated gastrointestinal (GI) model that was slightly modified from the method provided by ref. 26 Simulated Gastrointestinal Fluid (SGF) was prepared by dissolving 2 g per L NaCl, 7 mL per L HCl, and 3.2 g per L pepsin (porcine gastric mucosa) to achieve a pH of 1.2. For the gastric stage, 0.1 g of the oleogel sample was mixed with 15 mL of SGF. pH was adjusted and maintained at 2.0, and the mixture was incubated at 37 °C and rotated at 100 rpm for 2 hours to mimic stomach conditions, temperature, as well as peristaltic movement.

For the intestinal digestion phase, the pH of the mixture was adjusted to 7.0. Afterward, 3.5 mL of the extract solution of bile (54 mg mL^{-1}), 1.5 mL of salt solution ($CaCl_2$ 10 mM and NaCl 150 mM), and 2.5 mL of pancreatic lipase (75 mg mL^{-1} in phosphate buffer, pH 7.0) were added in sequence. The above blend was incubated at 37 °C and shaken at 100 rpm for another 2 hours under simulated intestinal digestion. For pH control at 7.0, 0.5 M NaOH was titrated in the system every 20 minutes for a period of 120 minutes.

Free fatty acid (FFA) release was assessed during the intestinal phase, and the total FFA release (%) was calculated by using the following formula:

$$\text{FFA released } (\%) = \frac{\text{NaOH volume} \times \text{NaOH molarity} \times \text{fish oil molecular weight}}{\text{powder mass} \times \text{LC} \times 2} \times 100 \quad (5)$$

where 868 g mol^{-1} represents the molecular weight of fish oil, and LC denotes the lipid content in the sample.

2.3 Statistical analysis

The experiments were carried out in triplicate and data were expressed as mean ± S.D. One-way ANOVA was performed, followed by Duncan's multiple range test to identify statistically significant differences among sample means. The statistical analysis was performed using SPSS software (version 25.0, SPSS Inc., Chicago, IL, USA), and $p < 0.05$ was considered statistically significant.

3 Results and discussion

3.1 Sustainable fish oil characterization

Tilapia fish oil (TFO) was extracted from byproducts utilizing a green process using natural deep eutectic solvents combined with ultrasonication, and was successfully extracted with high content of unsaturated fatty acids, especially omega-3 PUFA.[27] The extraction process achieved a yield of 27.73 g of oil per 100 g of viscera, surpassing the oil yield previously reported by the conventional method, with a yield of 6.27% from tilapia byproducts, underscoring its limited efficiency.[28] The enhanced recovery in the current method can be attributed to the mechanical effects of ultrasonication, where alternating compression and rarefaction waves induce cavitation, leading to cell membrane disruption and improved oil release.[29] The unsaturated fatty acid amounts were 74.07%, and they consisted of 42.35% MUFAs, 31.72% PUFAs, and the remaining 25.93% SFAs. The high unsaturated fatty acid content, notably omega-3 PUFAs, contains the most predominant omega-3 fatty

acids for 8.47% including α-linolenic acid (ALA, C18:3, *n*-3) for 1.86%, eicosatrienoic acid (C20:3, *n*-3) for 2.88%, eicosapentaenoic acid (EPA, C20:5, *n*-3) for 1.49%, docosapentaenoic acid (DPA, C22:5, *n*-3) for 0.81%, and docosahexaenoic acid (DHA, C22:6, *n*-3) for 1.44% and suggests that TVO has the potential to be a nutritionally useful oil source. The presence of SFAs, albeit being lower than that in typical fish oils, contributed to the structural stability of the resulting oleogels by promoting gel formation *via* their long aliphatic chains. Furthermore, TVO is suitable for usage in oleogel formulations due to its advantageous fatty acid composition, low processing, and ecologically friendly extraction.

3.2 Appearance, microstructure, porosity, and density of protein cryogels

The physical properties of cryogels play a fundamental role in determining their performance as oleogel matrices. In this

Table 2 Macroscopic appearance, scanning electron microscopy (SEM) micrographs, porosity (%), and density (g cm^{-3}) of protein cryogel formulations: WPI 20, WPI/FG 10 : 10, WPI 20–TA, WPI/FG 18 : 2-TA, WPI/FG 15 : 5-TA, and WPI/FG 10 : 10-TA[a]

	Protein cryogel	FESEM microstructure		Porosity (%)	Density (g cm^{-3})
WPI 20		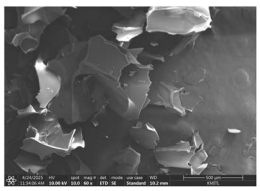	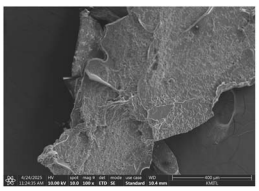	78.78 ± 0.11[a]	0.29 ± 0.06[c]
WPI/FG 10 : 10		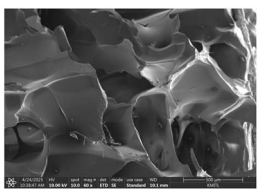	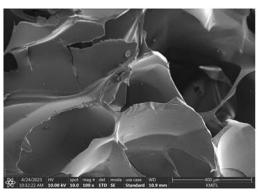	85.21 ± 0.16[a]	0.2 ± 0.02[c]
WPI 20–TA		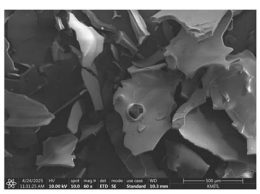	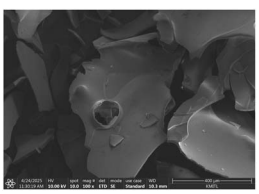	83.28 ± 0.92[b]	0.23 ± 0.01[c]
WPI/FG 18 : 2-TA		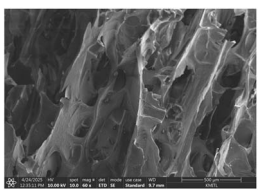	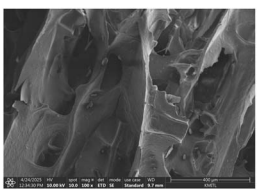	90.52 ± 0.25[c]	0.13 ± 0.02[b]
WPI/FG 15 : 5-TA		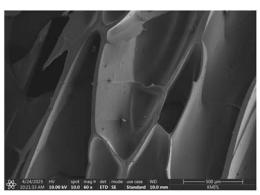	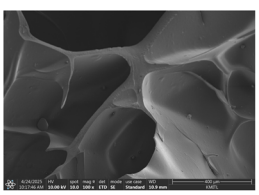	94.51 ± 0.11[d]	0.07 ± 0.04[a]
WPI/FG 10 : 10-TA		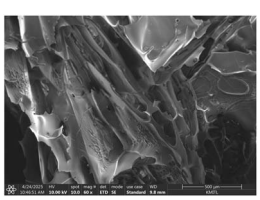	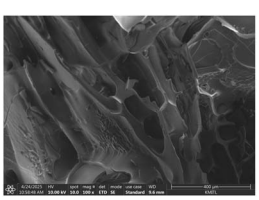	88.60 ± 0.77[c]	0.15 ± 0.03[b]

[a] Different superscript letters in the same column indicate significant differences ($p < 0.05$).

study, the appearance of the cryogels varied across formulations, as shown in Table 2. WPI 20 cryogels were irregularly shaped with flat surfaces, rough and sharp edges, meaning a loose network. Interestingly, the addition of tannic acid in WPI 20–TA reduced the surface roughness and gave a smoother and more compact structure, indicating more intermolecular interaction and partial crosslinking of protein chains. Cryogels with both WPI and FG, especially WPI/FG 10 : 10, were more homogeneous and slightly glossy. This is due to the synergistic effect of the two proteins forming a more uniform matrix. With

Table 3 Appearance, firmness, and color parameters (L^*, a^*, and b^*) of oleogel-structured composites loaded with omega-3 fatty acids from tilapia head fish oil, prepared using fish gelatin and whey protein-based cryogel particles, with and without tannic acid crosslinking[a]

			Color		
	Appearance oleogel	Firmness (N)	L^*	a^*	b^*
WPI 20	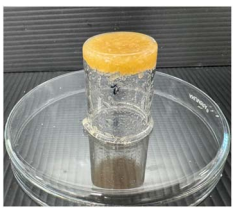	0.21 ± 0.07^{a}	51.01 ± 0.88^{b}	5.24 ± 0.80^{ab}	19.47 ± 0.30^{d}
WPI/FG 10 : 10	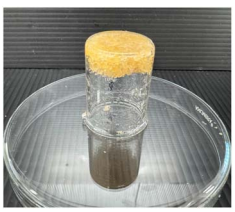	0.29 ± 0.23^{ab}	57.66 ± 0.69^{d}	4.68 ± 0.20^{a}	19.25 ± 0.48^{d}
WPI 20–TA	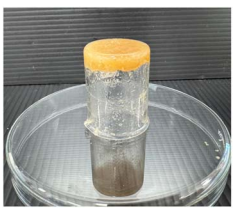	0.32 ± 0.12^{ab}	48.08 ± 1.40^{a}	6.09 ± 0.17^{b}	18.43 ± 0.31^{cd}
WPI/FG 18 : 2-TA	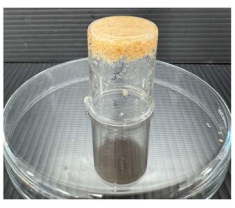	0.34 ± 0.18^{ab}	57.15 ± 0.65^{d}	6.1 ± 0.61^{b}	18.10 ± 0.28^{bc}
WPI/FG 15 : 5-TA	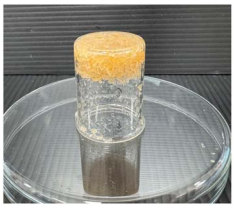	0.57 ± 0.20^{ab}	53.21 ± 0.52^{c}	6.03 ± 0.30^{b}	17.24 ± 0.16^{b}
WPI/FG 10 : 10-TA	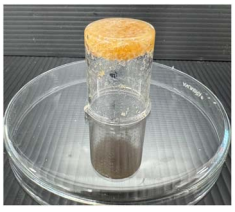	0.67 ± 0.16^{b}	47.25 ± 0.79^{a}	6.21 ± 025^{b}	16.04 ± 0.74^{a}

[a] Different superscript letters in the same column indicate significant differences ($p < 0.05$).

1% tannic acid (in WPI/FG 18 : 2-TA and WPI/FG 15 : 5-TA formulations), the gels became darker and more structured, which is likely due to protein–polyphenol interaction and hydrogen bonding.[10]

As shown in Table 2, freeze-dried cryogels showed significant differences in the microstructure among formulations. Freeze-drying induces pore formation through the sublimation of ice crystals.[30] WPI 20 was compact with poorly defined pores. WPI/FG 10 : 10 had larger and more open pores, indicating that FG blending led to more ice crystal formation and hence more porosity. Cryogels with tannic acid (*e.g.*, WPI/FG 15 : 5-TA and WPI/FG 18 : 2-TA) had a highly interconnected and regular pore structure with round pores. Tannic acid acted as a natural crosslinker, reinforcing the protein network and improving structural cohesion. These changes were associated with increased network rigidity and mechanical strength[31] and likely better oil immobilization in subsequent oleogel formation.

WPI and FG combination in the presence of TA also led to a more compact wall structure, reducing wall-to-wall distance and tightening the polymeric matrix. A clear inverse relationship was observed between porosity and density among the samples. WPI/FG 15 : 5-TA had the highest porosity (94.51%) and lowest density (0.07 g cm^{-3}), indicating a lightweight and highly porous network. Tannic acid contributed significantly to porosity enhancement due to increased protein–protein crosslinking and better freeze-drying efficiency. This porous structure is crucial for oil absorption capacity and stabilizing encapsulated oil in the cryogel network. This is consistent with previous reports that materials with higher porosity and lower density are favorable for oil entrapment and sustained release systems.[32] Moreover, pore morphology is important in defining compressive and mechanical properties; denser and more crosslinked structures provide better support for entrapped lipids or bioactives.[21] After being immersed in liquid oil, protein cryogels will gradually adsorb oil due to the pore structure: oil droplets come into contact with the pore channel on the surface of the cyrogel and were subject to capillarity, entering the pore structure, constantly filling the pores inside the aerogel and expelling air, and finally completing the transformation from a cyrogel into an oleogel.

3.3 Appearance, firmness, and color of oleogels

Appearance is an important property that influences consumer acceptability and product appeal. Firmness and color in this study varied oleogel formulation, particularly when fish gelatin (FG) and tannic acid (TA) were loaded with fish oil. WPI-only oleogels (WPI 20) were lighter yellowish in appearance, less firm (0.21 ± 0.07 N), and had comparatively moderate L^*, a^*, and b^* values that indicated pale and bright color ($L^* = 51.01 \pm 0.88$) as shown in Table 3. However, the incorporation of FG and TA made the color progressively darker and led to more mechanical strength. Notably, the WPI/FG 10 : 10-TA composition possessed the highest firmness value (0.67 ± 0.16 N), suggesting that the synergistic action among WPI, FG, and TA strengthened the cryogel structure network to improve the oil immobilization capacity and oleogel stability of the cryogels.[33] The increase in firmness was likely attributed to the high crosslinking density and the tight porous structure formed by the cryogelation process, which was confirmed by micromorphology analysis.

Regarding the colorimetric measurements, WPI/FG 10 : 10 exhibited the highest value of L^* (57.66 ± 0.69), reflecting a lighter hue compared to the other samples. Conversely, TA addition revealed a significant reduction in the value of L^*, particularly for WPI/FG 10 : 10-TA (47.25 ± 0.79), reflecting a darker color according to the intrinsic color of polyphenolic tannins. The a^* values increased when TA was incorporated, from 4.68 ± 0.20 to 6.21 ± 0.25, and the color turned into a redder tone. The b^* values decreased from 19.47 ± 0.30 for WPI 20 to 16.04 ± 0.74 for WPI/FG 10 : 10-TA, indicating a very slight reduction in the intensity of yellow. These results are in

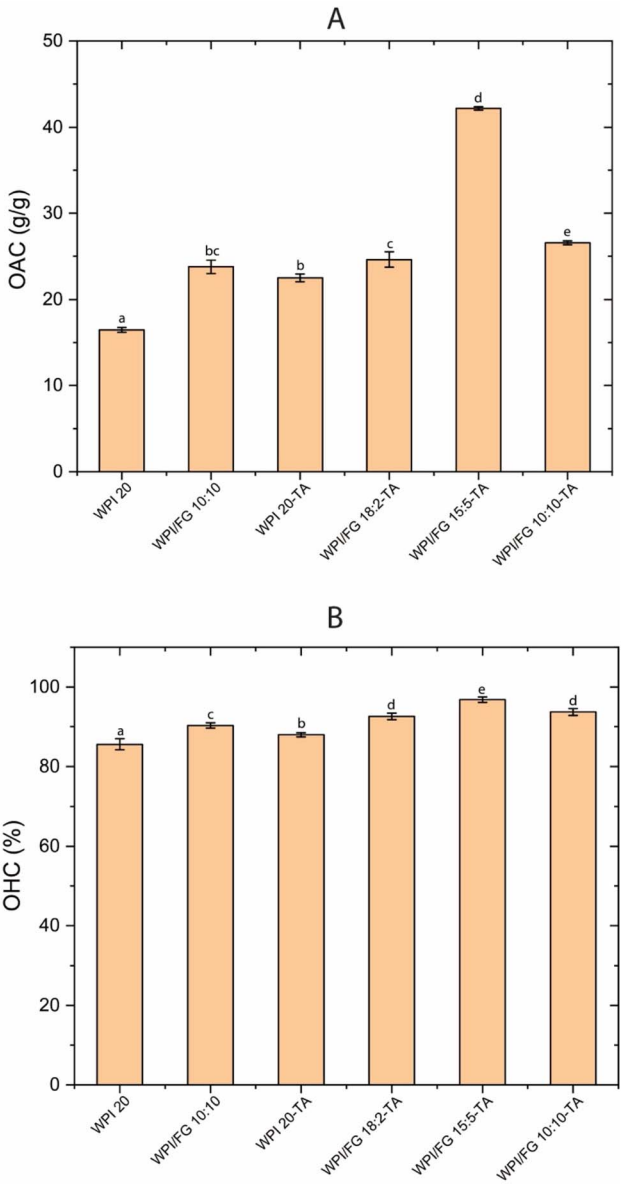

Fig. 1 (A) Oil absorption capacity (OAC) and (B) oil holding capacity (OHC) of cryogel-templated sustainable tilapia fish oil oleogels (STFOOs) formulated using whey protein isolate (WPI), fish gelatin (FG), and tannic acid (TA). Different superscript letters in the same column indicate significant differences ($p < 0.05$).

agreement with previous work wherein addition of polyphenolic compounds such as tannic acid affected sensory appearance as well as physical properties of gel-based systems due to their pigmentation and crosslinking potential.[10]

3.4 Oil absorption capacity (OAC) and oil holding capacity (OHC)

The ability of cryogels to absorb and retain oil is crucial in the creation of structurally stable and functional oleogels. Fig. 1 presents the OAC and OHC values of the cryogel particles that were formulated. Among all the samples, WPI/FG 15 : 5-TA had the highest oil absorption capacity (42.20 ± 0.20 g g^{-1}), significantly higher than that of other preparations ($p < 0.05$). Such improved performance can be attributed to the optimized biopolymer composition and reinforcing action of tannic acid, which in all probability enhanced the crosslinked structure and porosity and hence ensured greater oil entrapment. A similar trend was observed for oil holding capacity (OHC), with WPI/FG 15 : 5-TA showing maximum retention (96.80 ± 0.69%), suggesting better immobilization of oil even when subjected to the stress of centrifugation. The OHC values dropped with a rise in FG content, which might be due to the oil's ability to pass through its dense pores.[23] The OAC and OHC were obtained for WPI/FG 10 : 10-TA and were 26.72 ± 0.23 g g^{-1} and 93.69 ± 0.88%, respectively. These results indicate the beneficial effect of mixing WPI with FG in equal or near equal proportions, particularly with tannic acid, which leads to a denser and stronger cryogel matrix.[21]

Tannic acid addition significantly improved oil retention in WPI 20–TA and WPI/FG 18 : 2-TA compared to their respective control samples. This improvement is due to improved intermolecular interactions and the prevention of pore collapse during oil adsorption and centrifugation. Minimum OAC and OHC were observed in WPI 20 (16.47 ± 0.28 g g^{-1} and 85.58 ± 1.40%, respectively), indicating that WPI alone forms a less strong oil-holding network, which may be explained by its weaker internal structure and lower porosity. The findings are in consonance with previous communications where oil-related properties were enhanced by tannic acid-mediated crosslinking in hydrogel and cryogel platforms.[34] In general, the high OAC and OHC values are indicative that cryogel formulations, especially those with FG and TA, can serve as potential oil delivery systems for food, nutraceutical, and cosmetic applications.[24]

3.5 Oxidative stability of oleogels

The stability of the sustainable tilapia fish oil oleogel (STFO-O) against oxidation was assessed by tracking the peroxide value (PV) during storage for 8 days at 30 ± 1 °C, as depicted in Fig. 2. The peroxide value is a primary marker of lipid oxidation and reflects the sum of hydroperoxides as primary oxidation products. The peroxide value indicated an increasing pattern in all systems with respect to time, as expected for oxidative behavior in lipid-based systems. Among the samples, WPI 20 had the highest PV at day 8 (4.41 ± 0.19 meq per kg oil), indicative of a relatively poorer oxidation resistance. This can be because it has minimal physical barriers and antioxidant protection with regard to crosslinked or composite systems. Addition of fish gelatin (FG) to WPI/FG 10 : 10 reduced the PV to a lesser degree (3.99 ± 0.11 meq kg^{-1}), indicating that FG may be responsible for improved oxidative protection through improved gel structure and oil entrapment, inhibiting oxygen diffusion.[33] Significantly, TA-added samples had much better oxidative stability. WPI 20–TA, WPI/FG 18 : 2-TA, and WPI/FG 10 : 10-TA had much lower PV values after storage. Among them, WPI/FG 10 : 10-TA had the greatest oxidative stability under the lowest PV on day 8 (2.53 ± 0.11 meq per kg oil), followed by WPI/FG 15 : 5-TA (2.95 ± 0.14 meq per kg oil). This improved performance is

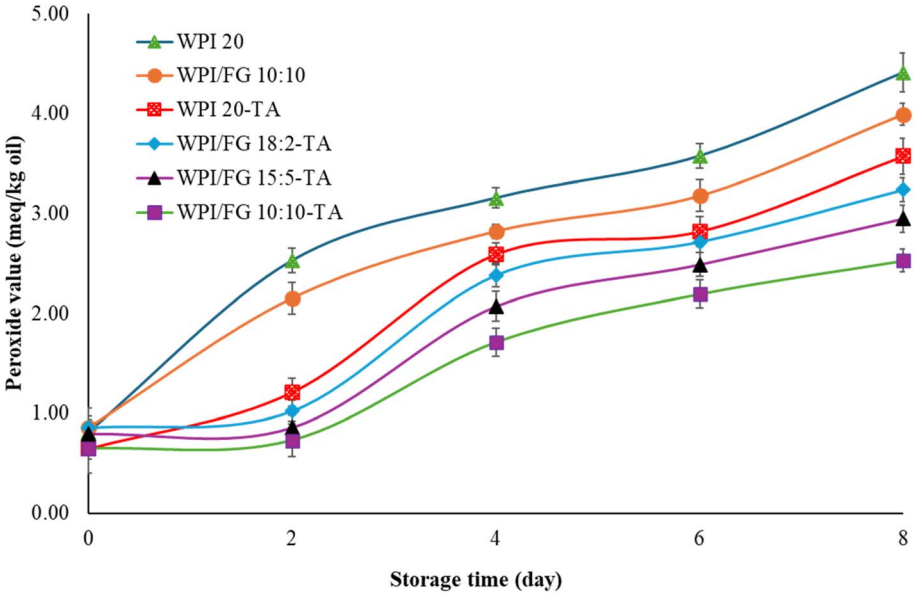

Fig. 2 PV of sustainable tilapia fish oil oleogel (STFO-O) formulations over 8 days of storage at 30 ± 1 °C. Samples include WPI 20, WPI/FG 10 : 10, WPI 20–TA, WPI/FG 18 : 2-TA, WPI/FG 15 : 5-TA, and WPI/FG 10 : 10-TA.

attributed to the synergistic effect of the interactions between the polyphenols and proteins in such a way that tannic acid stabilizes not only the cryogel network through hydrogen bonding but also serves as a natural antioxidant.[21] Tannic acid contains multiple phenolic hydroxyl groups, which can chelate pro-oxidant metal ions and scavenge free radicals so that lipid

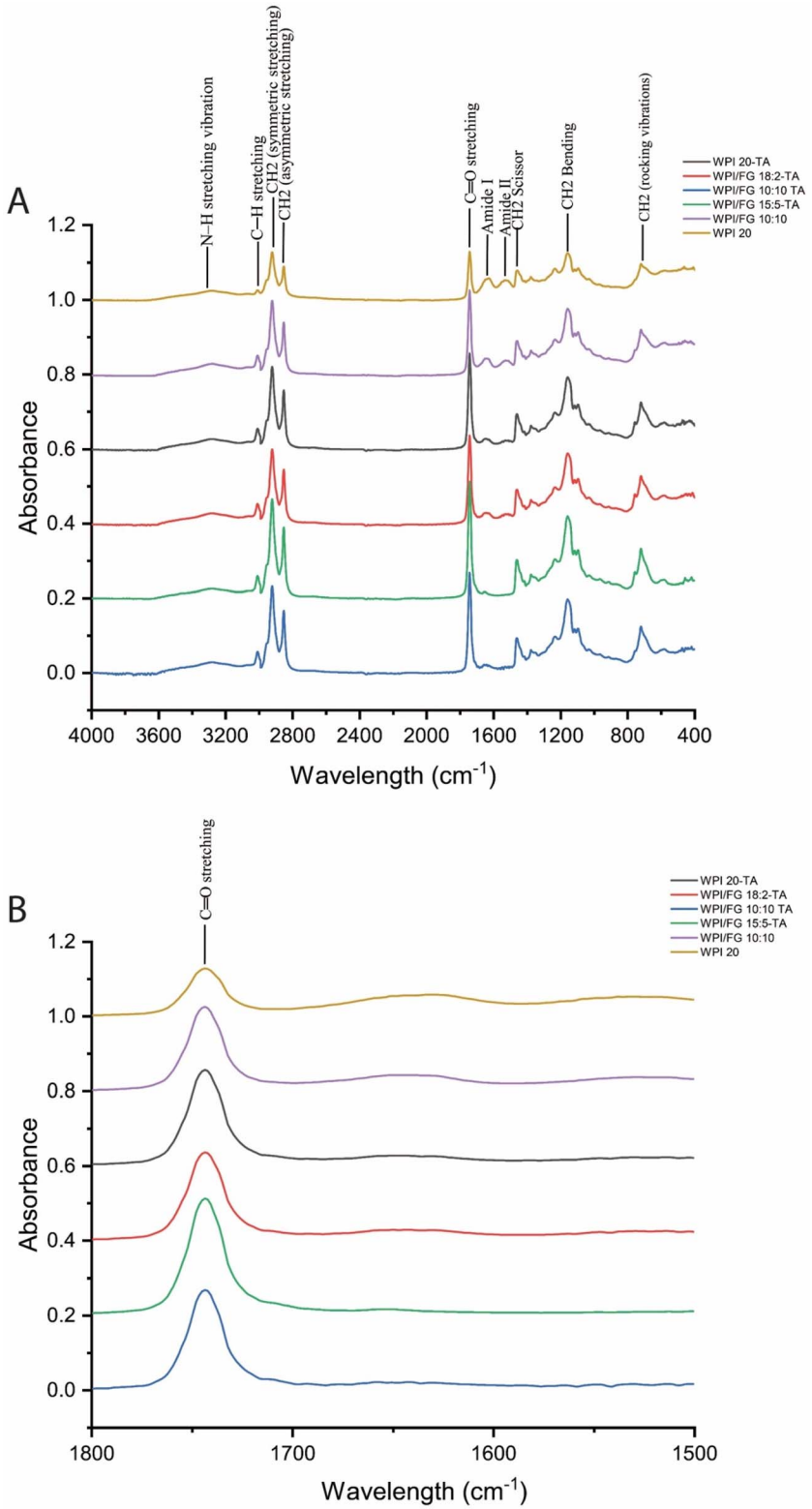

Fig. 3 (A) FTIR spectra of oleogels formulated using different cryogel matrices: WPI 20, WPI/FG 10 : 10, WPI 20–TA, WPI/FG 18 : 2-TA, WPI/FG 15 : 5-TA, and WPI/FG 10 : 10-TA. (B) Expanded FTIR spectra (1500–1800 cm^{-1}) showing detailed carbonyl and amide regions for oleogel formulations, highlighting the intensity variations in C═O stretching (1742 cm^{-1}) and protein structural changes.

oxidation is retarded.[35] The oxidative protection that is observed for WPI/FG 18 : 2-TA and WPI/FG 15 : 5-TA shows that increasing the ratio of WPI to FG creates a more structured matrix, which may offer a superior physical barrier to oxidative substances, with the balanced formulations such as 10 : 10 offering an intermediate balance between gel strength and antioxidant diffusion.

3.6 FTIR analysis of oleogels

FTIR spectroscopy was used to investigate the molecular interactions and structure of the protein-based cryogel oleogels with tilapia visceral oil, as shown in Fig. 3A. A broad peak at 3280 cm^{-1}, corresponding to the N–H stretching vibration (amide A), characteristic of proteins, was found in all the oleogel samples. In tannic acid (TA)-based formulations, there was an extra broadening or shoulder at 3330 cm^{-1}, which has been associated with O–H stretching vibrations for the phenolic hydroxyl moieties of TA. The merging of O–H and N–H bands suggests the establishment of hydrogen bonds between TA and the protein matrix, in line with the structural crosslinking and stability function of TA.[10] A unique absorption at 3004 cm^{-1} was observed that corresponds to C–H stretching vibrations of unsaturated fatty acids of the fish oil. Furthermore, strong CH_2 symmetric and asymmetric stretching vibrations were observed at 2918 and 2850 cm^{-1}, respectively. Such bands are typical for aliphatic chains of lipids and were most prominent in the WPI/FG 15 : 5-TA sample. This indicates a higher degree of oil entrapment and structural integration in this product. The carbonyl (C=O) stretching vibration at 1742 cm^{-1}, caused by ester linkages in triglycerides (fish oil), was present in all the samples but was most intense in WPI/FG 15 : 5-TA, which suggests better encapsulation of the oil (Fig. 3B). This band was, on the other hand, the least intense in WPI 20, which suggests lower oil loading and poor matrix–oil interaction. The coincidence of this peak with phenolic constituents of TA also speaks in favor of its contribution towards enhancing oil structuring in the protein network.[31,36]

Amide I (~1634 cm^{-1}) and amide II (~1523 cm^{-1}) bands, assigned to C=O or C–N stretching and peptide bond N–H bending or C–N stretching, respectively, were detected in all samples. Surprisingly, these bands were weaker and broader in TA-containing samples such as WPI/FG 15 : 5-TA and WPI/FG 10 : 10-TA than in WPI 20. Weakening and broadening of these bands can be attributed to protein unfolding and hydrogen bonding formation, which expose the buried functional groups and alter secondary structures.[30] The shifts in the spectra indicate a change towards more disordered (random coil) than ordered (α-helix, β-sheet) conformations, consistent with previous descriptions of polyphenol-induced denaturation and reorganization of proteins.[37] There were also minor peaks in all samples at 1456 cm^{-1} (scissoring of CH_2) and 1154 cm^{-1} (bending of CH_2), consistent with the presence of aliphatic hydrocarbon chains of lipids, consistent with fish oil composition.

3.7 *In vitro* digestion of oleogels

The *in vitro* digestion profiles of the oleogel samples were subjected to simulated gastrointestinal conditions, and the cumulative release of free fatty acids (FFAs) during the intestinal stage is shown in Fig. 4. The FFA release patterns of STFO-O were quite different between formulations under simulated intestinal digestion. In general, most of the samples exhibited an instantaneous release of FFAs during the first 20–40 minutes, followed by a sustained release phase that slowly declined to 120 minutes. This trend is in accordance with previous studies, where the matrix of an oleogel is demonstrated to degrade progressively, allowing lipase to catalyze the hydrolysis of the trapped fish oil.[38] The highest FFA release was at 120 minutes for WPI 20 (83.61 ± 1.42%), indicating the lowest resistance to lipolysis due to the simple form of the whey protein isolate

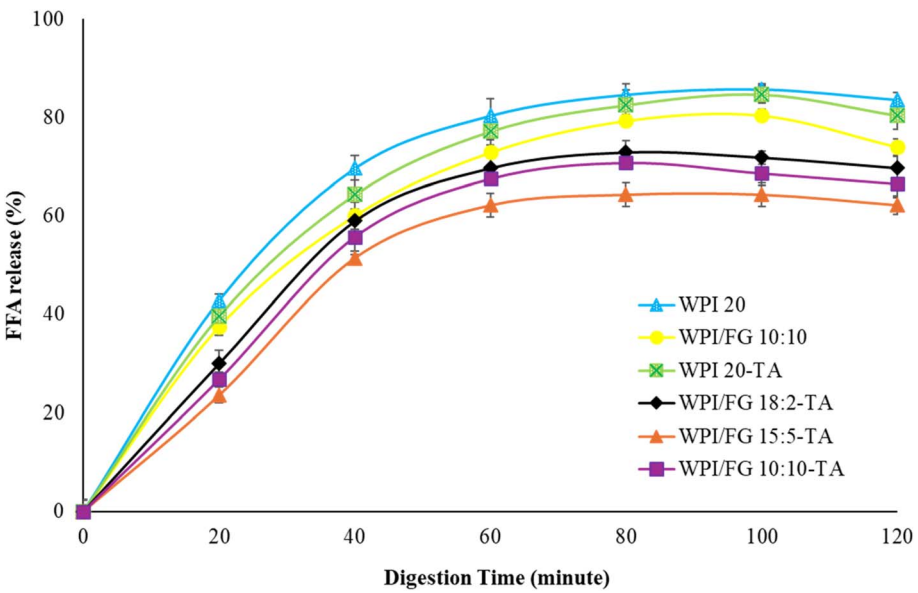

Fig. 4 FFA release of a sustainable tilapia fish oil oleogel during intestinal digestion.

(WPI) on its own. Similarly, high release (80.40 ± 1.66%) was also observed for WPI 20–TA, although lower than that of WPI 20, indicating that tannic acid can exhibit intermediate crosslinking properties whereby diffusion of the enzyme is affected to some extent.[39]

The addition of fish gelatin (FG) influenced the digestion behavior more significantly. WPI/FG 10 : 10 recorded reduced release (73.97 ± 2.90%), while WPI/FG 18 : 2-TA and WPI/FG 10 : 10 TA further diminished the FFA release to 69.68 ± 2.32% and 66.46 ± 1.85%, respectively. The latest release was found in WPI/FG 15 : 5-TA, which reached only 62.17 ± 2.76% at 120 minutes, displaying the strongest barrier function against enzymatic hydrolysis. The reduction of the FFA release with an increase in FG content and tannic acid addition can be understood based on the denser network architecture, enhanced intermolecular hydrogen bonding, and enhanced hydrophobicity of the cryogel matrix.[21] Such structural stability was ample enough to restrict access of digestive enzymes to the oil phase and thus modulate the lipid digestion process. An increase in the crosslinking level reduced lipase entry significantly and slowed the release of FFA.[40] Interestingly, the foregoing results highlight the gastrointestinal controllability of STFO-O systems. The amenability of FFA release modulation by varying protein type, proportion, and crosslink degree is not only beneficial for improving lipid bioavailability but also for the design of controlled delivery systems for functional food and nutraceutical products.

4 Conclusion and future perspectives

In this study, sustainable tilapia fish oil oleogels (STFO-O) were successfully developed using protein-based cryogel particles composed of whey protein isolate (WPI) and fish gelatin (FG), with and without tannic acid (TA) as a natural crosslinker. The resulting cryogels demonstrated diverse microstructures and porosities, which significantly influenced their oil absorption and holding capacities. Notably, formulations with optimized WPI/FG ratios and TA crosslinking (*e.g.*, WPI/FG 15 : 5 TA) exhibited stable structural integrity and the highest OAC and OHC, suggesting their strong potential as effective oleogel carriers. FTIR spectra confirmed the presence of hydrogen bonding interactions between protein matrices and fish oil components, as well as the characteristic absorption of tannic acid, supporting the structural and chemical integration of the oleogel system. Additionally, the oleogels showed improved oxidative stability compared to WPI/FG without natural antioxidants, attributed to the protective matrix that limited oxygen exposure and potentially leveraged the antioxidant properties of TA. The *in vitro* digestion study further demonstrated the ability of STFO-O to regulate lipid release during gastrointestinal simulation, indicating potential for targeted delivery and enhanced stability of omega-3 fatty acids. From a sustainability perspective, this approach valorizes approximately 30–40% of tilapia processing waste (viscera), potentially recovering 2–3% oil by weight. The use of natural crosslinkers eliminates synthetic additives, reducing chemical inputs by 100% compared to conventional oleogel systems. The green extraction method reduces solvent usage by 60% compared to traditional hexane extraction while maintaining comparable oil quality. Future research should focus on *in vivo* digestion studies to validate the controlled release benefits, pilot-scale processing optimization for commercial viability, and exploration of alternative natural crosslinkers to reduce dependence on tannic acid.

Data availability

The data that support the findings of this study are available from the corresponding author upon reasonable request. All data generated or analyzed during this study, including experimental results, analytical outputs, and figures, are included in this article.

Author contributions

Daniel Tua Purba: investigation, formal analysis, methodology, writing – original draft. Jaydeep Dave: investigation and writing, review & editing. Pichayada Somboon: supervision, validation, conceptualization, writing, review & editing.

Conflicts of interest

The authors declare that they have no known competing financial interests or personal relationships that could have appeared to influence the work reported in this paper.

Acknowledgements

The authors would like to thank the School of Food Industry, King Mongkut's Institute of Technology, Ladkrabang, for facility support. This work was supported by the King Mongkut's Institute of Technology Ladkrabang Research Fund under the KMITL Doctoral Scholarship [KDS2022/015].

References

1 O. Peñarubia, J. Toppe, M. Ahern, A. Ward and M. Griffin, *Rev. Aquacult.*, 2023, **15**, 32–40.
2 S. Bascuas, M. Espert, E. Llorca, A. Quiles, A. Salvador and I. Hernando, *LWT–Food Sci. Technol.*, 2021, **135**, 110228.
3 E. H. Fragal, L. Metilli, F. Pignon and S. Halila, *RSC Adv.*, 2025, **15**, 2988–2995.
4 M. C. Lee, X. Jiang, J. T. Brenna and A. Abbaspourrad, *Food Funct.*, 2018, **9**, 5598–5606.
5 A. R. Patel and K. Dewettinck, *Eur. J. Lipid Sci. Technol.*, 2015, **117**, 1772–1781.
6 A. Singh, F.-I. Auzanneau and M. Rogers, *Food Res. Int.*, 2017, **97**, 307–317.
7 A. J. Gravelle, G. G. B. Karatay and M. D. Hubinger, in *Advances in Oleogel Development, Characterization, and Nutritional Aspects*, Springer, 2024, pp. 231–269.
8 C. Francesco, P. Stella, R. Kato, V. B. Filip, D. Koen, M. Lara and C. Sonia, *Food Res. Int.*, 2024, **196**, 115029.

9 A. R. Taherian, M. Britten, H. Sabik and P. Fustier, *Food Hydrocoll.*, 2011, **25**, 868–878.
10 W. Miao, W. Zhou, D. J. McClements, Z. Zhang, Q. Lin, H. Ji, Z. Jin, S. Sang and C. Qiu, *Food Hydrocoll.*, 2025, **162**, 110903.
11 J. Pan, L. Tang, Q. Dong, Y. Li and H. Zhang, *Food Res. Int.*, 2021, **140**, 110057.
12 H. Qiu, K. Qu, H. Zhang and J.-B. Eun, *Food Hydrocoll.*, 2023, **142**, 108850.
13 M. C. Lee, X. Jiang, J. T. Brenna and A. Abbaspourrad, *Food Funct.*, 2018, **9**, 5598–5606.
14 N. Yu, W. Zuo, L. Ma, J. Yang and H. Katas, *Food Hydrocoll.*, 2024, **156**, 110265.
15 Y. Shi, J. Tang, W. Yan, Y. Liu, Y. Liu, H. Chen, C. Yang, C. Liu and R. Liang, *Food Chem.*, 2024, **454**, 139663.
16 A. Hayyan, A. V. Samyudia, M. A. Hashim, H. F. Hizaddin, E. Ali, M. K. Hadj-Kali, A. K. Aldeehani, K. H. Alkandari, H. T. Etigany and F. D. Alajmi, *Ind. Crops Prod.*, 2022, **176**, 114242.
17 E. A. Asevedo, B. M. E. das Chagas, S. D. de Oliveira Júnior and E. S. dos Santos, *Algal Res.*, 2023, **69**, 102940.
18 M. Betz, C. A. García-González, R. Subrahmanyam, I. Smirnova and U. Kulozik, *J. Supercrit. Fluids*, 2012, **72**, 111–119.
19 Y. Lin, H. Du, Y. Roos and S. Miao, *Food Hydrocoll.*, 2023, **143**, 108880.
20 I. Jung, B. Schroeter, S. Plazzotta, L. De Berardinis, I. Smirnova, P. Gurikov and L. Manzocco, *Food Hydrocoll.*, 2023, **142**, 108758.
21 J. Li, S. Zhao, Q. Zhu and H. Zhang, *Carbohydr. Polym.*, 2023, **315**, 120971.
22 A. Mohanan, Y. R. Tang, M. T. Nickerson and S. Ghosh, *RSC Adv.*, 2020, **10**, 14892–14905.
23 J. Li, Y. Sun, W. Shi, Y. Li, Y. Zou and H. Zhang, *Food Chem.*, 2024, **454**, 139804.
24 W. Ramadhan, A. N. Firdaos, W. V. Krisnawan, S. H. Suseno, B. Riyanto, W. Trilaksani and J. Santoso, *Sustainable Food Technol.*, 2024, **2**, 1022–1032.
25 S. Takeungwongtrakul and S. Benjakul, *J. Food Process. Preserv.*, 2017, **41**, e12876.
26 J. Peng, W. Zhang, Y. Zi, C. Shi, G. Kan, H. Gong, X. Wang and J. Zhong, *Food Hydrocoll.*, 2024, **152**, 109945.
27 A. Marsol-Vall, E. Aitta, Z. Guo and B. Yang, *Crit. Rev. Food Sci. Nutr.*, 2022, **62**, 2942–2962.
28 S. Kuepethkaew, S. Klomklao, N. Phonsatta, A. Panya and S. Benjakul, *Appl. Food Res.*, 2025, 100911.
29 J. Dave, N. Kumar, A. Upadhyay, D. T. Purba, T. Kudre, P. Nukthamna, S. Sa-nguanpuag, A. M. Moula Ali and S. C. B. Bavisetty, *Foods Raw Mater.*, 2024, 94–106, DOI: 10.21603/2308-4057-2025-1-627.
30 T. J. Silva, D. Barrera-Arellano and A. P. B. Ribeiro, *J. Food Sci.*, 2021, **86**, 2785–2801.
31 O. Mileti, D. Mammolenti, N. Baldino, F. R. Lupi and D. Gabriele, *Int. J. Biol. Macromol.*, 2024, **254**, 127973.
32 J. Li, C. Zhang, Y. Li and H. Zhang, *Carbohydr. Polym.*, 2022, **291**, 119603.
33 M. Abdollahi, S. A. H. Goli and N. Soltanizadeh, *Eur. J. Lipid Sci. Technol.*, 2019, **122**, 1900196.
34 C. Qiu, Y. Huang, A. Li, D. Ma and Y. Wang, *J. Agric. Food Chem.*, 2018, **66**, 13243–13252.
35 Z. Huang, L. Liao, D. J. McClements, J. Li, R. Li, Y. Zou, M. Li and W. Zhou, *LWT–Food Sci. Technol.*, 2022, **154**, 112814.
36 X. Liu, F. Xie, J. Zhou, J. He, Z.-u. Din, S. Cheng and J. Cai, *Food Hydrocoll.*, 2023, **142**, 108762.
37 T. Koupantsis, E. Pavlidou and A. Paraskevopoulou, *Food Hydrocoll.*, 2016, **57**, 62–71.
38 L. Dong, M. Lv, X. Gao, L. Zhang, M. Rogers, Y. Cao and Y. Lan, *Food Funct.*, 2020, **11**, 9503–9513.
39 Y. Guo, X. Yang, Y.-h. Bao, X.-l. Zhao, L. Huang, Z.-x. Chen, Y. Ma and W.-h. Lu, *LWT–Food Sci. Technol.*, 2022, **164**, 113660.
40 A. Ashkar, S. Laufer, J. Rosen-Kligvasser, U. Lesmes and M. Davidovich-Pinhas, *Food Hydrocoll.*, 2019, **97**, 105218.